Supporting information

Fergusonite - type rare earth niobates $ANbO_4$ (A = Nd, Sm, Eu) as electrode modifiers: Deep insight into A site variations towards bifunctional electrochemical sensing application

I. Jenisha Daisy Priscillal, Sea-Fue Wang, [a, *]

[a]Department of Materials and Mineral Resources Engineering, National Taipei University of Technology, No. 1, Sec. 3, Chung-Hsiao East Rd., Taipei 106, Taiwan.
Corresponding authors:

*S.-F. Wang, Email: sfwang@ntut.edu.tw

S1. Chemicals and reagents

Neodymium nitrate ($Nd(NO_3)_3$ ≥99% purity), Samarium nitrate ($Sm(NO_3)_3$ ≥99% purity), Europium nitrate ($Eu(NO_3)_3$ ≥99% purity), Niobium pentachloride (**(**$NbCl_5$≥99% purity), hydrogen peroxide (H_2O_2) and urea (CH_4N_2O) were purchased from Sigma Aldrich and carbon nanofibers (CNFs) were purchased from Rur-Grapheneox Company. All other necessary reagents and the above-mentioned chemicals have been used without further refinement. 0.1M (pH 7) phosphate buffer solution (PBS) prepared using sodium phosphate dibasic ($Na_2HPO_{4)}$ and sodium dihydrogen phosphate (NaH_2PO_4) had been used as supporting electrolytes in all electrochemical experiments. All the experiments used ultrapure fresh water obtained from a Millipore water purification system (Milli-Q, specific resistivity > 18MΩcm, S.A., Molsheim, France).

S2. Instrumentations

Phase configurational analysis was performed through X-ray diffraction (XRD), Rigaku D/maxB, and DMX-2200). X-ray photoelectron spectroscopy ESCA/Auger Laboratory (National Taiwan University, Taiwan) is applied to quantitatively analyze the chemical composition of the materials. The surface morphology and elemental composition of the as-prepared nanocomposite were studied employing high resolution (HR) transmission electron microscopy (H-7600, Hitachi-Japan) operating at 200 kV and scanning electron microscopy (SEM, Hitachi S4700) and energy dispersive X-ray (EDX, HORIBA EMAX XACT) spectroscopy. AC impedance spectroscopy was performed by Ω-metrohm autolab (AUT51770, 100-240V~ 75VA50/60 Hz). CHI 1205A

electrocatalytic work station was efficient to carry out the electrochemical measurements in three-electrode cells, as well as the amperometric method. Here, the modified GCE, saturated Ag/AgCl, and Pt wire were active as working, reference, and counter electrodes, respectively.

Table S1: Comparison of crystallographic properties.

Crystallites	**$NdNbO_4$**	**$SmNbO_4$**	**$EuNbO_4$**
Crystal type	Fergusonite	Fergusonite	Fergusonite
Crystal system	Monoclinic	Monoclinic	Monoclinic
Space group	I2	I2	I2
Space group number	5	5	5
a (Å)	5.4680	5.4210	5.3930
b (Å)	11.2800	11.1700	11.1300
C (Å)	5.1470	5.1200	5.1120
Lattice angles	α = γ =90°, β=94.7	α = γ =90°, β=94.7	α = γ =90°, β=94.7
Density (g/cm^3)	12.60	13.20	6.71
The volume of the cell (10^6 pm^3)	316.45	308.99	305.82
Crystal size (nm)	43.06	29.47	39.7

Table S2: Atomic % of Ln/Nb/O elements calculated from XPS and EDX

LnNbO4	Elements	Atomic% (From XPS)	Atomic% (From EDX)
NdNbO4	Nd	19.67	28.57
	Nb	15.01	14.64
	O	64.32	58.99
SmNbO4	Sm	12.99	27.35
	Nb	17.84	18.57
	O	69.17	54.08
EuNbO4	Eu	16.91	28.92
	Nb	17.32	10.91
	O	65.77	67.0

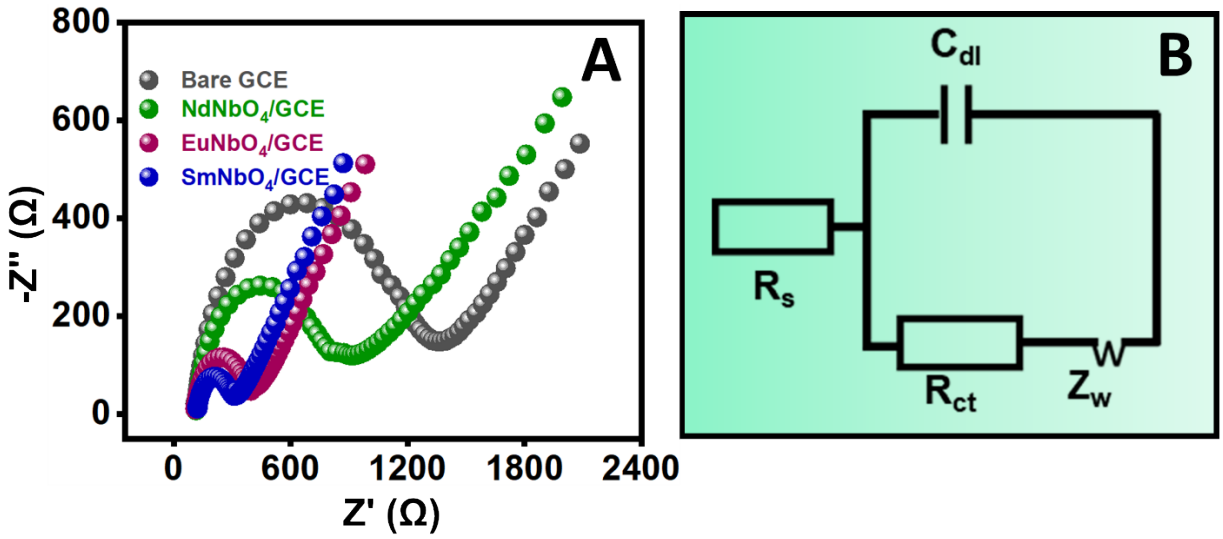

Figure S1: (A) Niquist plots corresponding to different electrodes; (B) Randel's equivalent circuit in EIS studies

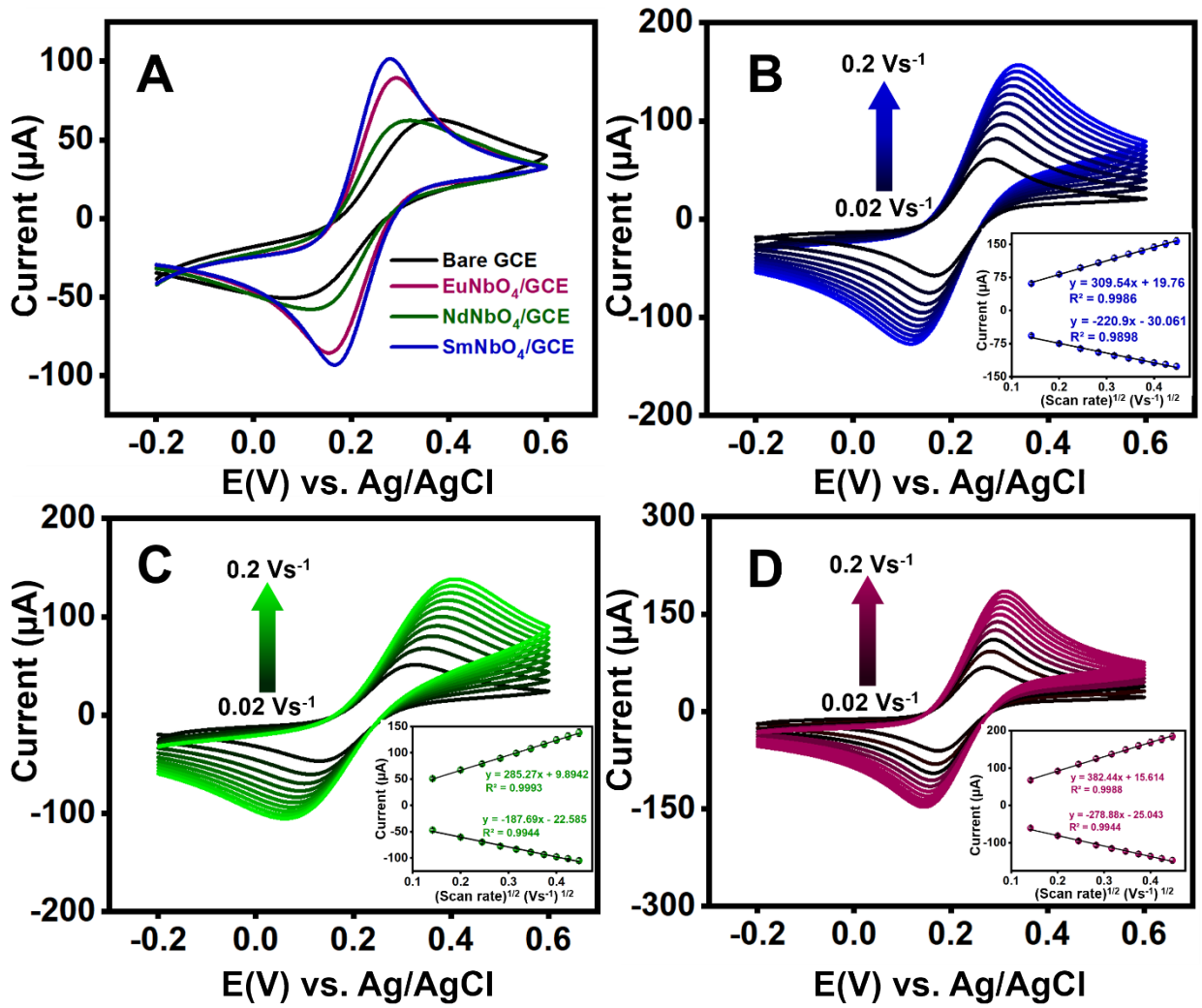

Figure S2: (A) Cyclic voltammograms for different electrodes (Bare and modified); CV profile of (B) $SmNbO_4$/GCE, (C) $NdNbO_4$/GCE (D) $NdNbO_4$/GCE for varying scan rates from 0.02-0.2 Vs^{-1} ; (Inset)Calibrated plot of the square root of scan rate versus anodic and cathodic peak currents; All the above experiments were performed in $[Fe(CN)_6]^{3-/4-}$in 0.1 M KCl as electrolyte.

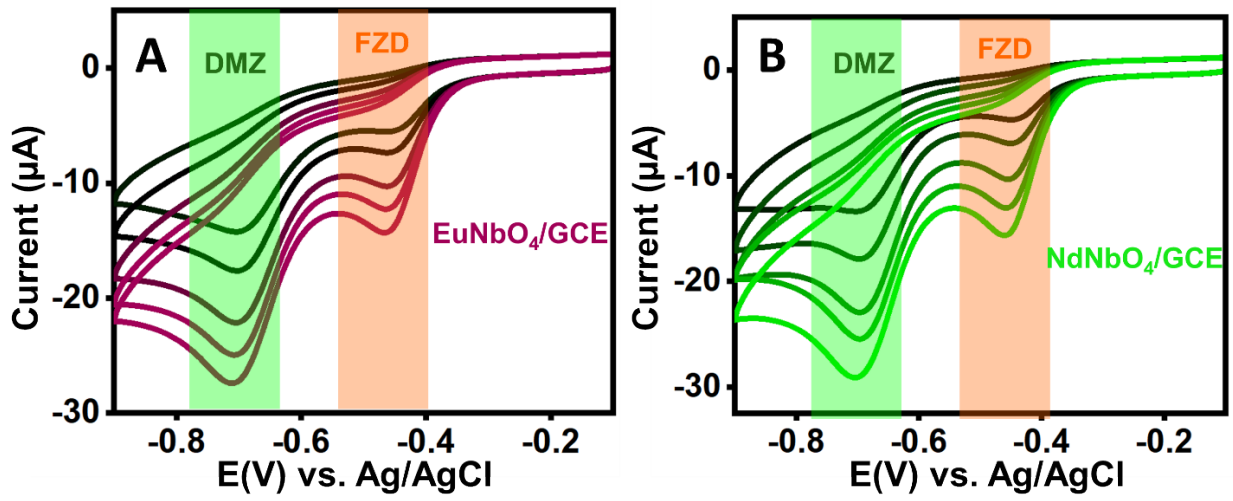

Figure S3: CV profile of 100 µM of FZD and DMZ at various $EuNbO_4$ and $NdNbO_4$ electrodes

Table S3: Comparison of previous literature about DMZ detection with the proposed $SmNbO_4$/GCE sensor.

Method	Electrode	Electrolyte	LOD (µM)	Linear range (µM)	References
[a]HPLC-UV	-	-	0.5	0–100	[1]
[b]GC-ECNI-MS	-	BSA		0.1–0.6	[2]
[c]LC-MS-MS	-	H_2O–CH_3CN	0.5	0–10	[3]
CV	μAg@[d]CPE	PB/7.0	0.6565	350–1	[4]
[e]DPSV	[f]MIS-CPE	PB/5.0	3.6	0.01–1	[5]
i-t	[g]rGO/[h]PB MCs/SPCE	PB/4.0	0.0032	0.02–1360	[6]
i-t	[i]MnT(*o*-glu)TTCl-[j]chit/GCE	BR/4.3	0.0027	1500–0.0027	[7]
LSV	Cu-Pd@[k]TLC/SPCE	PB/7.0	0.015	0.15–746.9	[8]
DPV	Mn-SnO@rGO/GCE	PB/7.0	0.002	0.009–1291	[9]
DPV simultaneous	**$SmNbO_4$/GCE**	**PB/7.0**	**0.004**	**0.01–264**	**This work**

[a]High-performance liquid chromatography-ultraviolet spectroscopy

[b]Gas chromatography–electron capture negative ionization mass spectrometry.

[c]Liquid chromatography-tandem mass spectrometry.

[d]Carbon paste electrode.

[e]Differential pulse stripping voltammetry.

[f]Molecularly imprinted siloxane.

[g]Reduced graphene oxide.

[h]Prussian blue microcubes.

[i]5,10,15,20-tetrakis[2-(2,3,4,6-tetraacetyl-β-D-glucopyranosyl)− 1-*O*-phenyl]porphyrin

[j]Chitosan

[k]teak leaves carbon

Table S4: Comparison of previous literature about DMZ detection with the proposed $SmNbO_4$/GCE sensor.

Method	Electrode	Electrolyte	LOD (µM)	Linear range (µM)	References
CV	[a]MWCNT/GCE	0.04 M/BR 6.0	2.30	3.0–800	[10]
DPV	MWCNT/GCE		0.080	0.49–59	[11]
[b]SWV	[c]SMDE	0.1 M/PB 6.0	0.023	0.088–3.99	[12]
[d]DPSV[g]	Gr/Au/GCE	0.04 M/BR 6.0	0.012	0.02–0.14; 0.14–400	[13]
I-T[f]	Gr/Au/GCE	0.04 M/BR 6.0	0.064	1.0–674.0	[13]
DPV	[e]GDS/GCE	0.05 M/PB 7.0	0.023	0.01–153.2	[14]
DPV	[f]BV/SPCE	0.05 M/PB 7.0	0.016	0.1–1189.8	[15]
DPV simultaneous	**$SmNbO_4$/GCE**	**PB/7.0**	**0.002**	**0.01–264**	**This work**

[a]Multiwalled carbon nanotube.

[b]Square wave voltammetric.

[c]Stationary mercury dropping electrode.

[d]Differential pulse stripping voltammetry.

[e]Gadolinium stannate

[f]Bismuth vanadate.

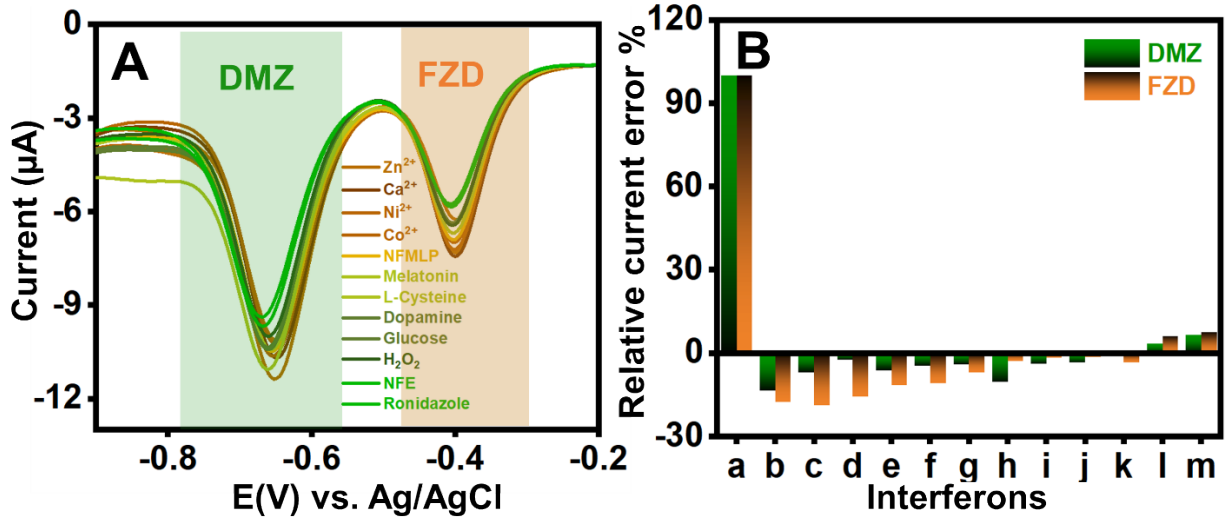

Figure S4: (C) Monitoring cathodic peak currents of FZD and DMZ in the presence of interfering compounds; (D) Plot of different interferon versus relative current error percentage.

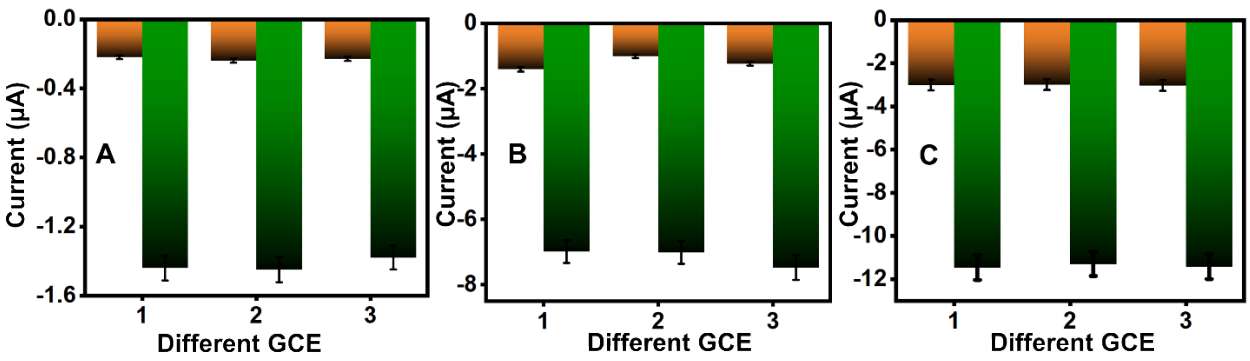

Figure S5: Reproducibility of $SmNbO_4$/GCE sensor using different GCE for (A) 10 µM, (B) 100 µM, and (C) 200 µM, of FZD and DMZ

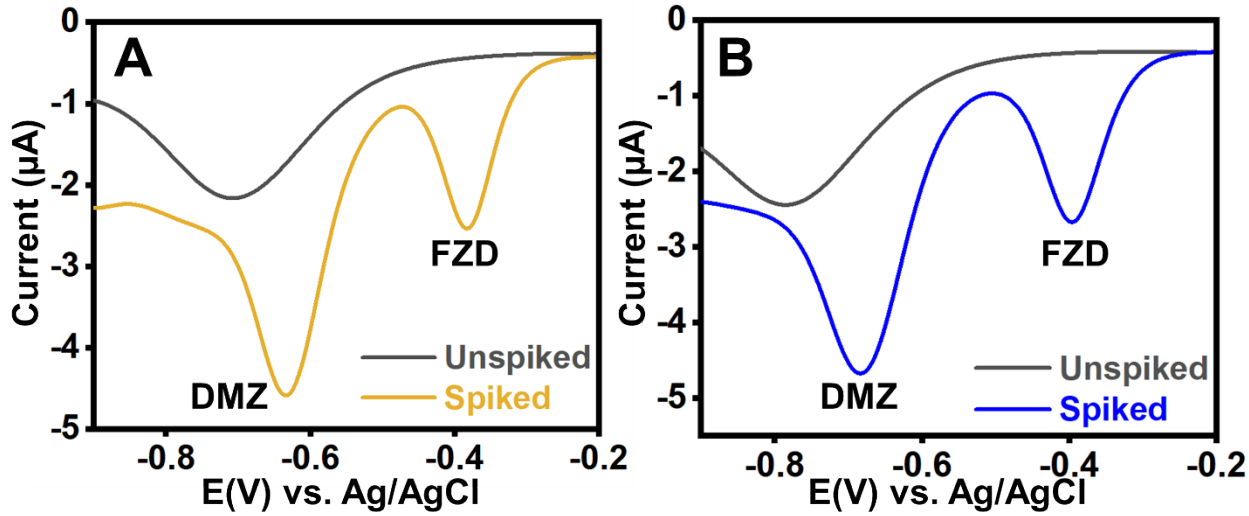

Figure S6: DPV analysis of FZD and DMZ in (A) saliva and (B) water samples medium (spiked and unspiked).

Table S5: RSD values of $SmNbO_4$/GCE sensor for different concentration of FZD and DMZ.

Concentration	RSD of FZD	RSD of DMZ
10 µM (Low)	0.66 %	0.78 %
100 µM (Medium)	1.64 %	3.88 %
200 µM(High)	4.34 %	2.66 %

Table S6: Real smaples with recovery percentage for DMZ and FZD

Samples	Analyte	Added (nM)	DPV Found (nM)	DPV Recovery (%)
Saliva sample	DMZ	0	0	-
		5	4.94	98.8 %
	FZD	0	0	-
		5	4.84	96.8 %
River Water	DMZ	0	0	-
		5	4.91	98.2 %
	FZD	0	0	
		5	4.77	95.4 %

References

1. Sams, M.J., Strutt, P.R., Barnes, K.A., Damant, A.P. and Rose, M.D., 1998. Determination of dimetridazole, ronidazole and their common metabolite in poultry muscle and eggs by high performance liquid chromatography with UV detection and confirmatory analysis by atmospheric pressure chemical ionisation mass spectrometry. *Analyst*, *123*(12), pp.2545-2549.
2. Ho, C., Sin, D.W., Wong, K.M. and Tang, H.P., 2005. Determination of dimetridazole and metronidazole in poultry and porcine tissues by gas chromatography–electron capture negative ionization mass spectrometry. *Analytica chimica acta*, *530*(1), pp.23-31.
3. Daeseleire, E., De Ruyck, H. and Van Renterghem, R., 2000. Rapid confirmatory assay for the simultaneous detection of ronidazole, metronidazole and dimetridazole in eggs using liquid chromatography-tandem mass spectrometry. *Analyst*, *125*(9), pp.1533-1535.

4. Zoubir, J., Bakas, I. and Assabbane, A., 2021. A simple platform for the electro-catalytic detection of the dimetridazole using an electrochemical sensor fabricated by electro-deposition of Ag on carbon graphite: application: orange juice, tomato juice and tap water. *Heliyon*, *7*(7), p.e07542.
5. Hu, C., Deng, J., Xiao, X., Zhan, X., Huang, K., Xiao, N. and Ju, S., 2015. Determination of dimetridazole using carbon paste electrode modified with aluminum doped surface molecularly imprinted siloxane. *Electrochimica Acta*, *158*, pp.298-305.
6. Keerthi, M., Akilarasan, M., Chen, S.M., Kogularasu, S., Govindasamy, M., Mani, V., Ali, M.A., Al-Hemaid, F.M. and Elshikh, M.S., 2018. One-pot biosynthesis of reduced graphene oxide/prussian blue microcubes composite and its sensitive detection of prophylactic drug dimetridazole. *Journal of The Electrochemical Society*, *165*(2), p.B27.
7. Gong, F.C., Wu, D.X., Cao, Z. and He, X.C., 2006. A fluorescence enhancement-based sensor using glycosylated metalloporphyrin as a recognition element for levamisole assay. *Biosensors and Bioelectronics*, *22*(3), pp.423-428.
8. Veerakumar, P., Koventhan, C. and Chen, S.M., 2023. Copper-palladium alloy nanoparticles immobilized over porous carbon for voltammetric determination of dimetridazole. *Journal of Alloys and Compounds*, *931*, p.167474.
9. Selvi, S.V., Rajaji, U., Chen, S.M. and Jebaranjitham, J.N., 2021. Floret-like manganese doped tin oxide anchored reduced graphene oxide for electrochemical detection of dimetridazole in milk and egg samples. *Colloids and Surfaces A: Physicochemical and Engineering Aspects*, *631*, p.127733.
10. Fotouhi, L., Nemati, M. and Heravi, M.M., 2011. Electrochemistry and voltammetric determination of furazolidone with a multi-walled nanotube composite film-glassy carbon electrode. *Journal of Applied Electrochemistry*, *41*(2), pp.137-142.
11. DUAN, L. and Zhang, L., 2012. Electrochemical behavior of furazolidone at mulit-walled carbon nanotubes modified glassy carbon electrode and its analytical application. *J. Anal. Sci*, *5*, pp.673-676.
12. Parham, H. and Esfahani, B.A., 2008. Determination of furazolidone in urine by square-wave voltammetric method. *Journal of the Iranian Chemical Society*, *5*(3), pp.453-457.

13. He, B.S. and Du, G.A., 2017. A simple and sensitive electrochemical detection of furazolidone based on an Au nanoparticle functionalized graphene modified electrode. *Analytical Methods*, *9*(30), pp.4341-4348.
14. Balamurugan, K., Rajakumaran, R., Chen, S.M., Chen, T.W. and Huang, P.J., 2021. Co-precipitation synthesis and characterization of rare-earth pyrochlore Gadolinium stannate; A novel electrocatalyst for the determination of furazolidone in water samples. *Int. J. Electrochem. Sci.*, *16*, p.210368.
15. Koventhan, C., Pandiyarajan, S. and Chen, S.M., 2022. Simple sonochemical synthesis of flake-ball shaped bismuth vanadate for voltammetric detection of furazolidone. *Journal of Alloys and Compounds*, *895*, p.162315.